Inorg. Chem. **2009**, *48*, 2985−2992

In Situ XRD, XAS, and Magnetic Susceptibility Study of the Reduction of Ammonium Nickel Phosphate $NiNH_4PO_4 \cdot H_2O$ into Nickel Phosphide

Gilles Berhault,*,† Pavel Afanasiev,† Hermione Loboué,† Christophe Geantet,† Tivadar Cseri,‡ Christophe Pichon,‡ Catherine Guillot-Deudon,§ and Alain Lafond§

Institut de Recherches sur la Catalyse et l'Environnement de Lyon, Université Lyon I, CNRS, 2 avenue Albert Einstein, 69626 Villeurbanne, France, IFP-Lyon, IFP, BP 3, 69390 Vernaison, France, and Institut des Matériaux Jean Rouxel, Université de Nantes, CNRS 2 rue de la Houssinière, BP 32229, 44322 Nantes Cedex 3, France

Received October 28, 2008

The reduction of the ammonium nickel phosphate $NiNH_4PO_4 \cdot H_2O$ precursor into nickel phosphide (Ni_2P), a highly active phase in hydrotreating catalysis, was studied using a combination of magnetic susceptibility and in situ X-ray diffraction and X-ray absorption spectroscopy (XAS) techniques. The transformation of $NiNH_4PO_4 \cdot H_2O$ into Ni_2P could be divided into three distinguishable zones: (1) from room temperature to 250 °C, the $NiNH_4PO_4 \cdot H_2O$ structure was essentially retained; (2) from 300 to 500 °C, only an amorphous phase was observed; (3) above 500 °C, a crystallization process occurred with the formation of Ni_2P. An in situ XAS study and magnetic susceptibility measurements clearly revealed for the first time that the amorphous region corresponds to the nickel pyrophosphate phase α-$Ni_2P_2O_7$. The phosphate reduction into phosphide did not start before 550 °C and led to the selective formation of Ni_2P at 650 °C.

1. Introduction

Sulfur-containing impurities present in fossil fuels are known to negatively impact the quality of air when burned in vehicles by producing sulfur oxides, a source of acid rain, or by inhibiting catalysts used in catalytic converters.[1] In the refining industry, hydrotreating processes are used to remove sulfur from petroleum feedstock generally using alumina-supported MoS_2-based catalysts promoted by Co or Ni.[2] In the last 10 years, more drastic regulations have been issued, leading to extensive research to improve the efficiency of hydrotreating catalysts. One way to achieve this goal is to develop a new generation of catalysts using active phases other than the commonly used MoS_2-based solids. In this respect, many studies have recently demonstrated that metal phosphides, and more specifically silica-supported nickel phosphide catalysts, could present hydrodesulfurization (HDS) activities superior to those of the commercial CoMo- or $NiMo/Al_2O_3$ sulfide catalysts.[3−7] Oyama et al. showed that Ni_2P/SiO_2 was more active than a $NiMo/Al_2O_3$ catalyst for HDS of dibenzothiophene and 4,6-dimethyldibenzothiophene, with the latter being a refractory sulfur compound commonly found in gas oils.[4,5]

Nickel phosphide catalysts are generally prepared by temperature-programmed reduction of ammonium nickel phosphate precursors under H_2 at relatively high temperature (600−650 °C).[8,9] However, even if this reductive treatment is of paramount importance to preparing highly active HDS nickel phosphide catalysts, only a few studies attempted to clarify the mechanism of reduction of the ammonium nickel phosphate precursor $NiNH_4PO_4 \cdot H_2O$ into Ni_2P.[10,11] On the basis of thermogravimetric analysis, Gopalakrishnan et al.

* To whom correspondence should be addressed. E-mail: gilles.berhault@ircelyon.univ-lyon1.fr. Phone: +33-472-44-53-20. Fax: +33-472-44-53-99.
† Université Lyon I.
‡ IFP-Lyon.
§ Université de Nantes.

(1) Hsu, C. S.; Robinson, P. R. *Practical Advances in Petroleum Processing*; Springer: Berlin, 2006.
(2) Topsøe, H.; Clausen, B. S.; Massoth, F. E. *Hydrotreating Catalysis—Catalysis, Science and Technology*; Springer-Verlag: Berlin, 1996.
(3) Sawhill, S. J.; Phillips, D. C.; Bussell, M. E. *J. Catal.* **2003**, *215*, 208.
(4) Oyama, S. T.; Wang, X.; Lee, Y. K.; Bando, K.; Requejo, F. G. *J. Catal.* **2002**, *210*, 207.
(5) Lee, Y. K.; Oyama, S. T. *J. Catal.* **2006**, *239*, 376.
(6) Zuzaniuk, V.; Prins, R. *J. Catal.* **2003**, *219*, 85.
(7) Shu, S.; Oyama, S. T. *Carbon* **2005**, *43*, 1517.
(8) Oyama, S. T.; Wang, X.; Lee, Y. K.; Chun, W. J. *J. Catal.* **2004**, *221*, 263.
(9) Wang, X.; Clark, P.; Oyama, S. T. *J. Catal.* **2002**, *208*, 321.
(10) Gopalakrishnan, J.; Pandey, S.; Kasthuri Rangan, K. *Chem. Mater.* **1997**, *9*, 2113.

10.1021/ic802074k CCC: $40.75
Published on Web 02/23/2009

systematically studied the formation of binary transition-metal phosphides (MoP, WP, Fe_2P, Ni_2P, FeP, RuP) through the reduction of their respective transition-metal phosphates.[10] The reduction of $NiNH_4PO_4 \cdot H_2O$ would occur through the formation of $NiHPO_4$ around 200 °C and of α-$Ni_2P_2O_7$ at 500 °C before obtaining Ni_2P at 800 °C. In a more recent study, Rodriguez et al. investigated the reduction of $NH_4NiPO_4 \cdot H_2O$ into Ni_2P using in situ X-ray diffraction (XRD).[11] They observed first that, around 400 °C, the sample became totally amorphous before the appearance of diffraction lines for Ni_2P between 650 and 800 °C. α-$Ni_2P_2O_7$ was only observed when $NiNH_4PO_4 \cdot H_2O$ was heated in a pure stream of He instead of H_2, while $NiHPO_4$ was never obtained. Moreover, the exact nature of the amorphous phase observed was not determined. Therefore, the mechanism of reduction of ammonium nickel phosphate into nickel phosphide is not clarified yet. Moreover, Rodriguez et al.[11] surprisingly found a quite different reduction process for silica-supported systems passing through the intermediate formation of metallic nickel and of poor HDS-active Ni-rich phosphide phases like $Ni_{12}P_5$.[12] This different reduction process would suggest an influence of the nature of the support on the reduction behavior. It is therefore essential to reinvestigate the reduction of $NH_4NiPO_4 \cdot H_2O$ into Ni_2P without any possible support interference to get new information about the mechanism of reduction of this ammonium nickel phosphate into nickel phosphide by combining in situ XRD, X-ray absorption spectroscopy (XAS), and magnetic susceptibility studies.

2. Experimental Section

Synthesis. Unsupported Ni_2P was obtained by H_2 reduction of the $NiNH_4PO_4 \cdot H_2O$ precursor. Therefore, in a first step, $NiNH_4PO_4 \cdot H_2O$ was prepared by precipitation from an aqueous solution using a method derived from that of Carling et al.[13] A 20-mL aqueous solution containing 12.6 mmol of $Ni(NO_3)_2 \cdot 6H_2O$ (Aldrich, 99.9 %) and an excess of $(NH_4)_2HPO_4$ (89.3 mmol; Aldrich, >98 %) was stirred for 48 h at 90 °C, yielding a greenish-yellow precipitate. This solid was collected by filtration and dried at 100 °C for 24 h. The specific Brunauer−Emmett−Teller (BET) surface area was 11 $m^2\ g^{-1}$. The $NiNH_4PO_4 \cdot H_2O$ precursor was then reduced into Ni_2P under H_2 at 650 °C (H_2 flow = 150 mL min^{-1}; heating rate = 2 °C min^{-1}).

For comparison purposes, a pure crystalline Ni_2P compound was synthesized from the elements through a solid-state reaction route. A mixture of Ni and P in a stoichiometric ratio was put in an evacuated, sealed, fused silica tube. The tube was heated at 900 °C (20 °C h^{-1}) for 4 days and then cooled down to room temperature (100 °C h^{-1}). The obtained powder was homogeneous and well-crystallized. The BET specific surface area was 5 $m^2\ g^{-1}$.

Characterization Methods. Raman spectra were recorded with a Raman Jobin Yvon, Labram HR800 spectrometer. The 514 nm excitation wavelength of an Ar−Kr laser was focused using a 50× objective. The laser power on the samples was typically 4 mW. Wavenumber measurements were accurate within ca. 3 cm^{-1}.

^{31}P NMR spectra were obtained with an Avance DSX-400 Bruker spectrometer equipped with a magic-angle-spinning (MAS) probe. The ^{31}P NMR frequency was 161.9 MHz, and 85% phosphoric acid was used as an external reference. The samples were packed into a 4-mm-diameter rotor and spun respectively at 8.5 and 10 kHz for the phosphate and phosphide solids. Spectra were acquired using a single 1.8-μs pulse (flip angle = $\pi/4$; recycle time = 1 s). The measurements were performed at room temperature with 2000 scans. Using the *Winfit* software,[14] the ^{31}P NMR shift anisotropy of the Ni_2P sample was determined from the spinning-sideband intensities in the MAS spectra using the method of Herzfeld and Berger.[15]

XRD patterns of the $NH_4NiPO_4 \cdot H_2O$ precursor and of Ni_2P were obtained with the use of a D8 Bruker diffractometer equipped with a Ge monochromator (Cu Kα_1 radiation) set up in a Bragg−Brentano geometry and with a Vantec fast detector. The powder patterns were recorded in the range $2\theta = 5-100°$ with 0.017° 2θ steps. The Rietveld refinements were carried out with the help of the program *JANA2000*.[16]

In situ XRD measurements were performed on a Panalytical X'Pert Pro MPD θ/θ diffractometer equipped with a curved graphite monochromator using Cu Kα radiation. The reaction cell (XRK 900 Anton Paar) was equipped with an open holder allowing gas to pass through the sample. The H_2 flow was adjusted at 20 mL min^{-1}. Temperature-programmed reduction was performed as follows: heating ramp = 2 °C min^{-1} from room temperature to 650 °C with 65-s dwells of 50 °C each.

Extended X-ray absorption fine structure (EXAFS) experiments were carried out at the X1 Beamline of the HASYLAB facility (Hamburg, Germany) using the synchrotron radiation from the DORIS III ring running at 4.45 GeV (with positrons) with an average current of 120 mA. The Ni K-edge at 8333 eV was monitored in the transmission mode with three ion chambers as detectors (measuring the intensity before and after the sample and a metallic Ni foil reference). The signal-to-noise ratio was optimized by acquiring multiple scans for each spectrum. To characterize the Ni environment evolution during reduction treatments, a dedicated cell for in situ measurements was used.[17] The ammonium nickel phosphate compound was reduced up to 500 °C (heating rate = 5 °C min^{-1}; H_2 flow = 50 mL min^{-1}). After a dwell of 30 min at a given temperature of reduction, a series of three spectra was acquired with an acquisition time of 30 min per spectrum. EXAFS analysis was performed using the Athena−Artemis software package.[18] EXAFS data fitting used theoretical backscattering phases and amplitudes calculated with FEFF6 code.[19]

Magnetization measurements were performed in the range 5−300 K under an applied field of 200 Oe by means of a Quantum Design MPMS SQUID magnetometer. About 50 mg of a powdered sample was placed inside a gelatin capsule, whose the contribution (less than 10% at room temperature) was subtracted from the overall signal. Because the compositions of the samples prepared via the soft chemistry route are not well-known, we could not calculate the molar susceptibilities of these compounds. Thus, the measured magnetic moment was not corrected from the electron-core contribution, and we calculated the mass susceptibility. On the other hand, the crystalline Ni_2P sample prepared at high temperature was found to be pure. Thus, it was possible to calculate the molar susceptibility.

(11) Rodriguez, J. A.; Kim, J. Y.; Hanson, J. C.; Sawhill, S. J.; Bussell, M. E. *J. Phys. Chem. B* **2003**, *107*, 6276.
(12) Sawhill, S. J.; Layman, K. A.; Van Wyk, D. R.; Engelhard, M. H.; Wang, C.; Bussell, M. E. *J. Catal.* **2005**, *231*, 300.
(13) Carling, S. G.; Day, P.; Visser, D. *Inorg. Chem.* **1995**, *24*, 3917.
(14) Massiot, D.; Thiele, H.; Germanus, A. *Bruker Rep.* **1994**, *140*, 43.
(15) Herzfeld, J.; Berger, A. E. *J. Chem. Phys.* **1980**, *73*, 6021.
(16) Petricek, V.; Dusek, M. *Z. Kristallogr.* **2004**, *219*, 692.
(17) Geantet, C.; Soldo, Y.; Glasson, C.; Matsubayashi, N.; Lacroix, M.; Proux, O.; Ulrich, O.; Hazemann, J. L. *Catal. Lett.* **2001**, *73*, 95.
(18) Ravel, B.; Newville, M. *J. Synchrotron Radiat.* **2005**, *12*, 537.
(19) Rehr, J. J.; Albers, R. C. *Rev. Mod. Phys.* **2000**, *72*, 621.

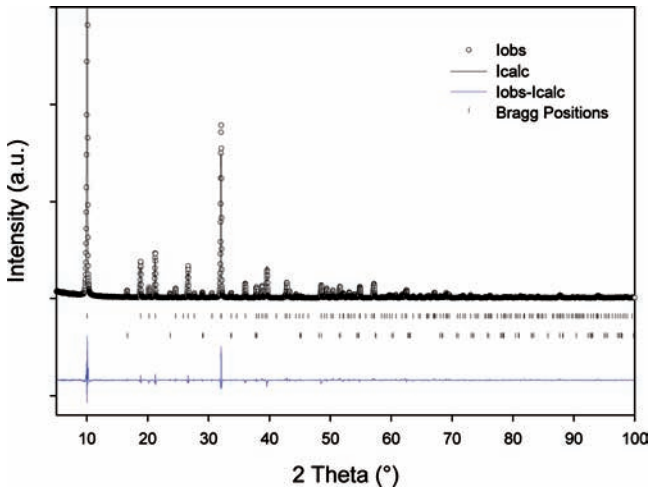

Figure 1. XRD pattern of the $NiNH_4PO_4 \cdot H_2O$ precursor. Rietveld refinement was performed using the structural model of Carling et al.[13]

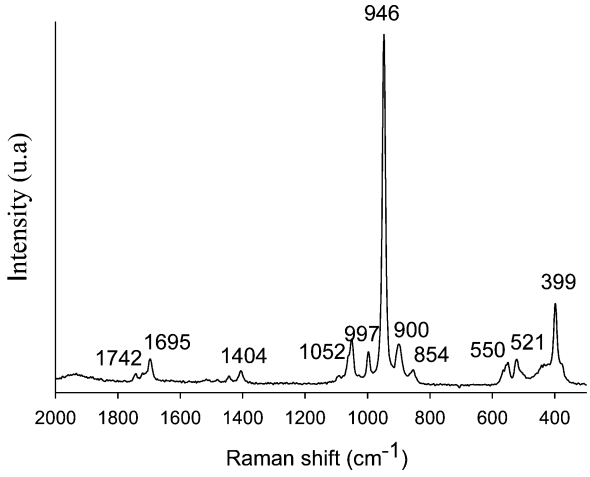

Figure 2. Raman spectrum of the $NiNH_4PO_4 \cdot H_2O$ precursor.

3. Results

3.1. Characterization of the $NiNH_4PO_4 \cdot H_2O$ Precursor. Figure 1 displays the XRD pattern of the $NiNH_4PO_4 \cdot H_2O$ precursor. The main diffraction peaks were assigned to JCPS Card No. 00-050-0425. Moreover, in order to determine the degree of purity of our starting phosphate material, a Rietveld refinement was also performed using the structural model proposed by Carling et al.[13] The starting material was found to be relatively homogeneous, with only a small quantity of $(NH_4)_2HPO_4$ (less than 4%) as impurity.

The $NiNH_4PO_4 \cdot H_2O$ precursor was also characterized using laser Raman spectroscopy (Figure 2) and ^{31}P NMR (Figure S1 in the Supporting Information). The Raman spectrum shows an intense band at 946 cm^{-1} due to the symmetric PO_2 stretching vibration.[20] The 399 cm^{-1} band is attributed to the symmetric PO_2 bending mode.[20,21] The 521 and 550 cm^{-1} bands are ascribed to PO_2 antisymmetric bending modes, while the 997 and 1052 cm^{-1} signals are related to PO_2 antisymmetric stretching modes. It is worth noting that nickel nitrate (used to synthesize $NiNH_4PO_4 \cdot H_2O$) would also exhibit an intense band at 1050 cm^{-1} due to a symmetric stretching mode of vibration of the nitrate moiety.[22] However, in such a case, a bending mode of vibration would be expected at 720 cm^{-1}, which is not detected here. Therefore, nitrate impurities are not detected on the $NiNH_4PO_4 \cdot H_2O$ precursor sample. The NH_4 group gives rise to antisymmetric and symmetric bending modes of vibration respectively at 1404, 1443, and 1481 cm^{-1} and at 1695 and 1742 cm^{-1}. Libration modes of the water molecule are observed at 900 and 854 cm^{-1}.

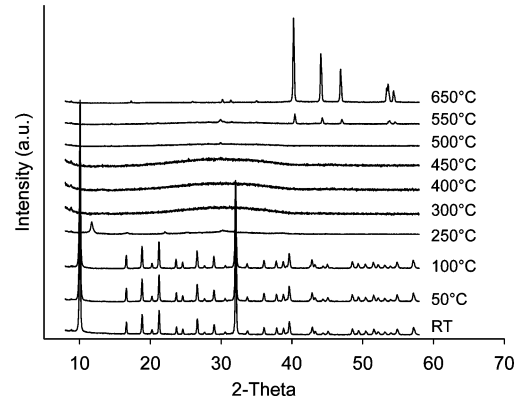

Figure 3. Evolution of the XRD patterns during the reduction of $NiNH_4PO_4 \cdot H_2O$ into Ni_2P. Reduction was performed under a H_2 flow of 20 mL min^{-1} from room temperature to 650 °C. The reduction process presents three distinguishable zones: (1) from room temperature to 250 °C, $NiNH_4PO_4 \cdot H_2O$ was still detected; (2) from 300 to 500 °C, only amorphous phases were observed; (3) above 500 °C, a crystallization process occurred, leading to Ni_2P.

The ^{31}P NMR spectrum of the initial compound presents an isotropic chemical shift at 1 ppm with three series of sidebands extending on a chemical shift range -160 ppm $< \delta < +160$ ppm. This NMR signature is characteristic of a $NH_4H_2PO_4$ (or here $NiNH_4PO_4$) type structure.[23]

3.2. Reduction of $NiNH_4PO_4 \cdot H_2O$ into Ni_2P. In Situ XRD and ^{31}P MAS NMR. The H_2 reduction process of the $NiNH_4PO_4 \cdot H_2O$ precursor into Ni_2P was followed in situ by recording X-ray patterns from room temperature up to 650 °C each 50 °C. Figure 3 reports the evolution of the diffractograms during the reduction into nickel phosphide. Up to a reduction temperature of 200 °C, $NiNH_4PO_4 \cdot H_2O$ is still detected even if the intensity of the diffraction peaks decreases for temperatures higher than 100 °C. At 250 °C, only weak diffraction peaks can be observed, corresponding to a mixture of different ammonium or nickel polyphosphate phases and nickel pyrophosphate as well. However, an exact assignment of the different diffraction peaks remains challenging. Only, the (100) reflection of ammonium hydrogen phosphate $NH_4H(PO_3)_2$ (at $2\theta = 11.7°$, JCPDS 045-0004) is clearly assigned. This species would result from the elimination of NH_3 and H_2O from the $(NH_4)_2HPO_4$ impurity according to the following equation:

(20) Lu, G.; Li, C.; Wang, W.; Wang, Z.; Guan, J.; Xia, H. *Mater. Sci. Eng. B* **2005**, *116*, 47.
(21) Cahil, A.; Najdoski, M.; Stefov, V. *J. Mol. Struct.* **2007**, *834*, 408.
(22) Carter, C.; Khulbe, P. K.; Gray, J.; Van Zee, J. W.; Angel, S. M. *Anal. Chim. Acta* **2004**, *514*, 241.
(23) Gunter, G. C.; Craciun, R.; Tam, M. S.; Jackson, J. E.; Miller, D. J. *J. Catal.* **1996**, *164*, 207.

$$2(NH_4)_2HPO_4 \rightarrow NH_4H(PO_3)_2 + 3NH_3 + 2H_2O \quad (1)$$

Moreover, a broad signal without any detectable peaks around $2\theta = 30°$ suggests the beginning of an amorphization process. At 300 °C, the XRD pattern does not present any discernible peak, confirming the formation of an amorphous phase, which is detected up to 500 °C. At this temperature, a crystallization process begins that is characterized by the appearance of very weak diffraction peaks of $Ni(PO_3)_2$.

At 550 °C, the $Ni(PO_3)_2$ phase progressively disappears, while Ni_2P is now detected (Figure 4). However, the XRD profile still presents some amorphous character characterized by a broad peak in the 30–40° 2-θ range. After reduction at 650 °C, only intense diffraction peaks of the Ni_2P phase are detected. Complementary elemental analysis confirmed the selective formation of Ni_2P at this temperature of reduction (Ni, 66.7 atom %; P, 33.3 atom %).

The ^{31}P NMR spectrum of this sample (Figure S2 in the Supporting Information) shows two groups of signals centered on isotropic chemical shifts of 1488 and 4076 ppm characteristic of Ni_2P, which contains two types of P atoms.[24] Other nickel phosphide phases (like $Ni_{12}P_5$) were not detected. No signals could be detected anymore in the −160 ppm < δ < +160 ppm range, showing the disappearance of any phosphate impurities. ^{31}P NMR results therefore confirm the selective formation of Ni_2P. Moreover, using the *Winfit* software,[14] the center bands with the sideband patterns were fitted in order to determine the chemical shift anisotropy δ_{CSA}, the asymmetry parameter η, and the linewidths of the isotropic chemical shifts. The results are compared in Table 1 with those reported by Stinner et al. for Ni_2P/SiO_2.[24] Isotropic chemical shifts as well as the ^{31}P shift anisotropy parameters (δ_{CSA} and η) are quite close to those reported for Ni_2P/SiO_2, suggesting that the electronic environments around the two types of P sites are very similar on unsupported Ni_2P and on Ni_2P/SiO_2. Only the asymmetry parameter η associated with the isotropic chemical shift at 4076 ppm presents a lower value than that on Ni_2P/SiO_2. Consequently, these results confirm that the silica support did not perturb the electronic properties of Ni_2P.

Finally, it should be underlined that the BET specific surface area initially of 11 $m^2\ g^{-1}$ progressively decreases to 9, 5, and 4 $m^2\ g^{-1}$ after reduction at 300, 400, and 650 °C, respectively.

In Situ XAS. The evolution of the XRD profile during in situ reduction of $NiNH_4PO_4 \cdot H_2O$ into Ni_2P evidenced the formation of an amorphous phase between 300 and 500 °C. In order to get complementary information about the nature of this amorphous phase, the reduction of the $NiNH_4PO_4 \cdot H_2O$ compound was followed by in situ XAS spectroscopy. The ammonium nickel phosphate compound was then reduced up to 500 °C. Figure 5 shows the evolution of the absorption spectra at the Ni K-edge during the $NiNH_4PO_4 \cdot H_2O$ reduction. The analysis of the X-ray absorption near-edge structure (XANES) spectra shows a marked decrease of the white-line intensity as soon as the reduction temperature reaches 200 °C. The white-line signal corresponds to a Ni 1s → Ni 4p transition and is an indirect measure of the density of the final states located above the Fermi level.[25,26] Above 200 °C, the white line remains significant even if its intensity hardly changes up to 500 °C (Figure 6). Comparison with a Ni_2P reference presenting negligible white-line intensity (Figure 5) therefore suggests that the oxygen environment around the Ni absorber atom of the initially nonreduced ammonium nickel phosphate does not disappear after reduction in the 200−500 °C temperature range. However, reduction at 200 °C already modifies the electronic structure of the phosphate compound through a noticeable decrease of the density of states above the Fermi level.

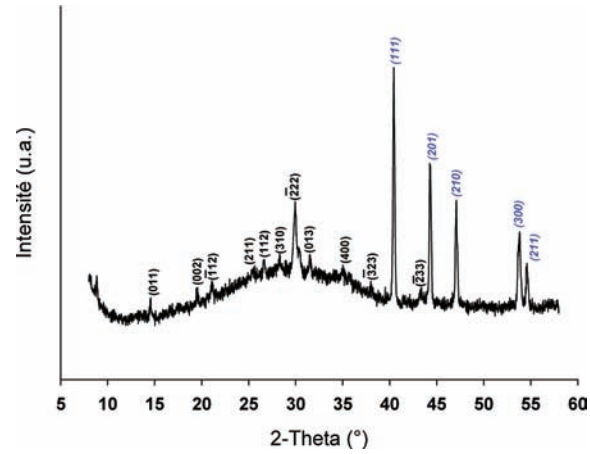

Figure 4. XRD pattern obtained after reduction at 550 °C of the $NiNH_4PO_4 \cdot H_2O$ precursor. The main diffraction peaks are indexed: $Ni(PO_3)_2$ (black); Ni_2P (blue, italic).

Table 1. ^{31}P MAS NMR Results for the Ni_2P Sample Obtained by the Reduction of $NiNH_4PO_4 \cdot H_2O$ at 650 °C[a]

sample	ν_{rot} (kHz)	δ_{iso} (ppm)	fwhm (kHz)	δ_{CSA} (ppm)	η
Ni_2P (this study)	10	1488	0.6	−278	0
		4076	2.0	−78	0.35
Ni_2P/SiO_2[24]	10	1487	1.0	−271	0
		4081	2.5	−73	0.85

[a] The results are compared to those of Ni_2P/SiO_2.[24]

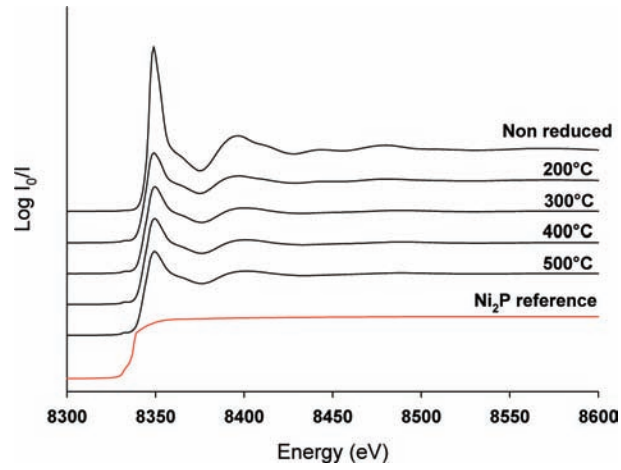

Figure 5. Evolution of the edge region of the XAS spectra at the Ni K-edge during the reduction of $NiNH_4PO_4 \cdot H_2O$ up to 500 °C.

(24) Stinner, C.; Tang, Z.; Haouas, M.; Weber, T.; Prins, R. *J. Catal.* **2002**, *208*, 456.

(25) Chen, J. C. *Surf. Sci. Rep.* **1997**, *30*, 1.

(26) Bart, J. C. J. *Adv. Catal.* **1986**, *34*, 203.

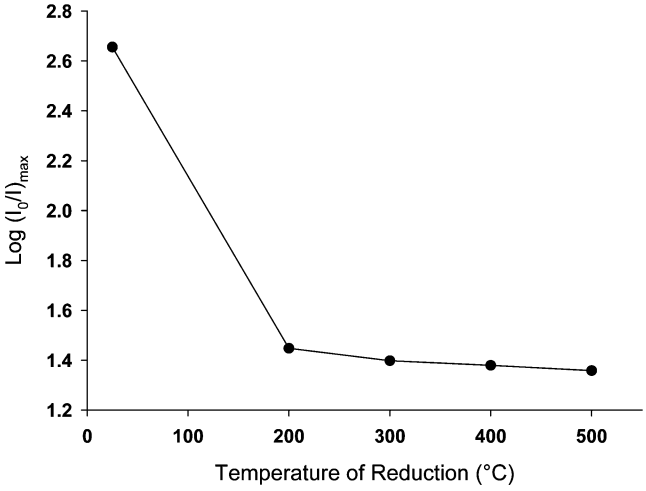

Figure 6. Evolution of the white-line intensity at the Ni K-edge during the reduction of $NiNH_4PO_4 \cdot H_2O$ up to 500 °C.

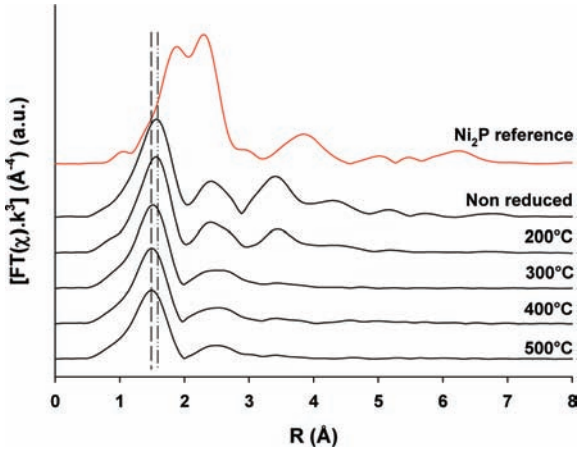

Figure 7. FTs of the EXAFS spectra at the Ni K-edge during the reduction of $NiNH_4PO_4 \cdot H_2O$ up to 500 °C. Comparison to a well-crystallized Ni_2P reference.

Figure 7 reports the Fourier transforms (FTs) of EXAFS spectra at the Ni K-edge for the initial $NiNH_4PO_4 \cdot H_2O$ compound and after reduction at 200, 300, 400, and 500 °C. The FT EXAFS spectra of the initial $NiNH_4PO_4 \cdot H_2O$ solid corresponds to a well-ordered state with four distinguishable peaks assigned respectively to Ni−O (first peak), Ni−P (second peak), and Ni−Ni (third and fourth peaks) shells. After reduction at 200 °C, the FT spectrum remains essentially the same even if the solid appears slightly less ordered. For temperatures of reduction of 300 °C or higher, crystalline order for distances higher than 3 Å could not be found anymore. Moreover, a slight shift of the first peak toward lower distances is observed. These results suggest a less ordered structure at long distances. This is in agreement with in situ XRD results showing the formation of an amorphous phase in this 300−500 °C temperature range. The absence of any change in the FT profiles of the EXAFS spectra above 300 °C also clearly underlines a weak (if any) modification of the solid that remains at a phosphate state. After reduction at 500 °C, comparison with a Ni_2P reference definitely confirms the absence of any phosphide contribution (Figure 7).

The EXAFS spectra were simulated using amplitude and phase shift functions calculated by FEFF for the $NH_4NiPO_4 \cdot H_2O$ reference determined by Carling et al.[13]

Table 2. Curve-Fitting Results of the First Backscattered Ni−O Shell of the $NiNH_4PO_4 \cdot H_2O$ Compound during Its Reduction up to 500 °C[a]

temperature of reduction/°C	CN	R/Å	$\sigma^2 \times 10^3$/Å^2	ΔE_0/eV	QF[b]
RT	6.0 f	2.06 ± 0.03	3	2.27	1.00
200	5.8 ± 1.3	2.05 ± 0.02	11 ± 3	2.42	0.14
300	5.3 ± 0.8	2.01 ± 0.01	12 ± 2	4.70	0.33
400	5.2 ± 0.7	2.01 ± 0.01	13 ± 2	5.36	0.40
500	5.1 ± 0.6	2.01 ± 0.01	14 ± 1	5.07	0.21

[a] CN = coordination number; f = fixed; S_0^2 is fixed at 0.8. [b] The quality factor (QF) or reduced χ^2 function is defined as $N/\nu m\sum_{i=1}^{m}[(d_i - t_i)/(\varepsilon_i)]^2$ where $N = 2\Delta k\Delta R/\pi$ = number of independent parameters, $\nu = N - P$ = number of degrees of freedom (with P = number of parameters varied in the fit), m = number of data points, d_i = experimental data points, t_i = fit points, and ε_i = individual errors of the experimental data points.

Fitting was only performed on the first backscattered Ni−O shell because we were not able to simulate the second shell, which may contain close contributions of different backscattering atoms. The Ni−O contribution was fixed at six O atoms for the initial sample. Table 2 summarizes the EXAFS curve-fitting results for the initial $NiNH_4PO_4 \cdot H_2O$ compound and after reduction at 200, 300, 400, and 500 °C.

The Ni−O distance slightly decreases between 200 and 300 °C, while it remains constant for higher temperatures of reduction. Similarly, after a slight decrease from 5.8 to 5.3 when going from 200 to 300 °C, the coordination number hardly changes after reduction in the 300−500 °C reduction temperature domain. Moreover, the complementary EXAFS analysis of the sample reduced at 500 °C after cooling to room temperature reveals that the thermal disorder does not lead to the disappearance of the third coordination sphere even if it decreases the amplitude of the FT peaks. The amorphous state therefore corresponds to a well-dispersed system with nondetectable Ni−Ni contributions. The absence of any long-order distance and the low specific surface area (9 m^2 g^{-1}) after reduction at 300 °C suggest that a nickel phosphate glass structure was formed.

Therefore, the EXAFS analysis confirms that, in the 300−500 °C temperature domain, the amorphous phase observed by XRD still corresponds to the oxygen environment of a nickel phosphate compound.

Magnetism. Like many nickel salts, the ammonium nickel phosphate has a Curie−Weiss behavior at least for temperatures above 10 K.[13] Because the nickel phosphides have totally different magnetic behavior, the magnetic measurements allow the evolution of the nickel environment from the phosphate compounds to the phosphide compounds to be followed.

Figure 8 shows the mass susceptibility and the reciprocal mass susceptibility of compounds for a set of reduction temperatures. The compounds reduced at 250 and 500 °C keep a Curie−Weiss-type magnetic behavior. The molar Curie constant for nickel compounds containing Ni^{II} in an octahedral environment is about 1.4 emu K^{-1}(mol of Ni)$^{-1}$, corresponding to a mass Curie constant of 2.3 × 10^{-3} emu K^{-1} (g of Ni)$^{-1}$.[27,28] Assuming that the magnetic behavior of the studied compounds is only due to the presence of

(27) Escobal, J.; Pizarro, J. L.; Mesa, J. L.; Rojo, J. M.; Bazan, B.; Arriortua, M. I.; Rojo, T. *J. Solid State Chem.* **2005**, *178*, 2626.
(28) Carlin, R. L.; De Jongh, L. J. *Chem. Rev.* **1986**, *86*, 659.

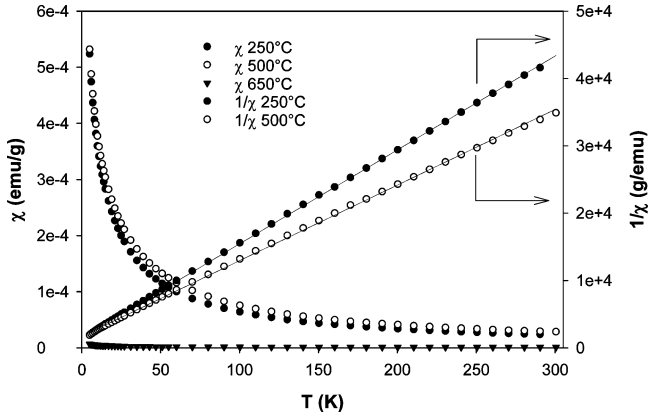

Figure 8. Thermal variation of χ and $1/\chi$ after reduction of the $NiNH_4PO_4 \cdot H_2O$ compound at different temperatures.

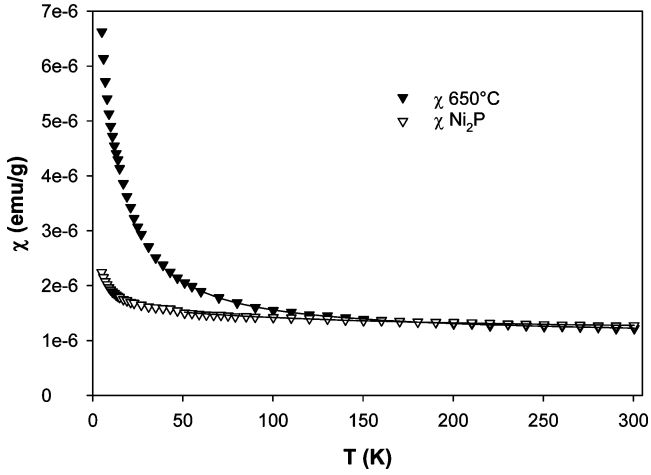

Figure 9. Magnetic susceptibilities of the phosphate compound after reduction at 650 °C compared to that of the crystalline Ni_2P compound.

isolated Ni^{2+}, one can deduce the Ni mass content of the sample from the mass susceptibility versus temperature curve. The decrease of the slope of the $1/\chi$ curves is due to the increase of the Curie constant from 7.2×10^{-3} emu K^{-1} g^{-1} at 250 °C to 8.9×10^{-3} emu K^{-1} g^{-1} at 500 °C corresponding to the increase of the nickel content from 31% to 39%. It is worth noting that the Ni content is 31% in $NiNH_4PO_4 \cdot H_2O$ and 40% in α-$Ni_2P_2O_7$. The formation of the nickel pyrophosphate α-$Ni_2P_2O_7$ after reduction at 500 °C would then be in agreement with that of Gopalakrishnan et al.[10] Thus, the amorphization process observed between 300 and 500 °C corresponds to the transformation of the starting material $NiNH_4PO_4 \cdot H_2O$ into α-$Ni_2P_2O_7$ by the loss of NH_3 and H_2O but not of PH_3.

A dramatic change of the magnetic behavior of the studied compounds is observed between 500 and 650 °C. For the compound treated at 650 °C, the magnetic susceptibility is by far lower than the expected value for a temperature-dependent paramagnetic behavior. Indeed, Figure 9 compares the magnetic susceptibility of this compound with that of the crystalline pure Ni_2P.

Both compounds have a nearly temperature-independent paramagnetism, with the same TIP value of 1.1×10^{-6} emu g^{-1}, likely due to delocalization of the electrons, giving a metallic behavior.[29,30] The small increase of the susceptibility at low temperature was due to a very small quantity of magnetic impurity corresponding to less than 0.5 wt % of Ni^{2+}.[31]

4. Discussion

The use of nickel phosphide as a very active phase for a new generation of hydrotreating catalysts has generated in the last years a strong research effort to optimize its preparation.[12,32,33] Even if a few studies have recently tried to promote alternative low-temperature routes for the preparation of Ni_2P,[34−36] the traditional method of preparation still requires a high-temperature treatment under H_2 from ammonium nickel phosphate precursors. However, the mechanism of formation of such a nickel phosphide phase has been rarely studied. Using thermogravimetric analysis, Gopalakrishnan et al.[10] proposed that $NiNH_4PO_4.H_2O$ would transform into $NiHPO_4$ around 200 °C, while around 500 °C, α-$Ni_2P_2O_7$ would be formed. Reduction of this nickel pyrophosphate phase would then occur. Using in situ XRD, Rodriguez et al.[11] only observed the formation of an amorphous phase around 400 °C followed by the appearance of Ni_2P at 650 °C. α-$Ni_2P_2O_7$ would only be formed from $NiNH_4PO_4 \cdot H_2O$ through an inert treatment under He at 600 °C. In order to clarify the mechanism of reduction of $NiNH_4PO_4 \cdot H_2O$ into Ni_2P, a combined in situ XRD, XAS, and magnetic susceptibility study was herein performed.

Our in situ XRD study confirms that the synthesis of Ni_2P from the ammonium nickel phosphate precursor passes through the intermediate formation of an amorphous phase between 300 and 500 °C, as was already observed by Rodriguez et al.[11] However, contrary to the mechanism proposed by Gopalakrishnan et al.,[10] the formation of $NiHPO_4$ was not detected before the amorphization of the sample. The XAS and magnetic susceptibility measurements were then performed to better characterize the nature of the intermediate amorphous phase. EXAFS and XANES results at the Ni K-edge undoubtedly identified the nickel environment in the amorphous region as the one expected for a nickel phosphate compound. However, the progressive amorphization process between 200 and 300 °C seems to be accompanied by a modification of the nickel phosphate structure. Indeed, after reduction at 200 °C, FT EXAFS profiles (Figure 7) and curve-fitting results (Table 2) suggest that the $NiNH_4PO_4 \cdot H_2O$ phase was essentially retained at this temperature of reduction even if XANES results already revealed a modification of the electronic structure of this

(29) Ishida, S.; Asano, S.; Ishida, J. *J. Phys. F: Met. Phys.* **1987**, *17*, 475.
(30) Shirotani, I.; Takahashi, E.; Mukai, N.; Nozawa, K.; Kinoshita, M.; Yagi, T.; Suzuki, K.; Enoki, T.; Hino, S. *Jpn. J. Appl. Phys.* **1993**, *32*, 294.
(31) Zeppenfeld, K.; Jeitschko, W. *J. Phys. Chem. Solids* **1993**, *54*, 1527.
(32) Wang, A.; Ruan, L.; Teng, Y.; Li, X.; Lu, M.; Ren, J.; Wang, Y.; Hu, Y. *J. Catal.* **2005**, *229*, 314.
(33) Shu, Y.; Oyama, S. T. *Carbon* **2005**, *43*, 1517.
(34) Yang, S.; Liang, C.; Prins, R. *J. Catal.* **2006**, *237*, 118.
(35) Henkes, A.; Schaak, R. E. *Chem. Mater.* **2007**, *19*, 4234.
(36) Loboué, H.; Guillot-Deudon, C.; Popa, A. F.; Lafond, A.; Rebours, B.; Pichon, C.; Cseri, T.; Berhault, G.; Geantet, C. *Catal. Today* **2008**, *130*, 63.

phosphate compound. The complete amorphization of the sample after reduction at 300 °C was accompanied by a slight shift to lower Ni−O distances and a lower coordination number as well. Above 300 °C and up to 500 °C, the EXAFS and XANES results did not show any noticeable further modification of the phosphate compound. The combination of an amorphous state and a low surface area suggests that the nickel phosphate sample presents a glass structure.

Magnetic susceptibility measurements confirmed the maintenance of a phosphate state characterized by a Curie−Weiss-type magnetic behavior between 250 and 500 °C. The increase in the nickel content deduced from the Curie constant at 250 and 500 °C, however, strongly suggests a modification of the nickel phosphate phase between these two temperatures of reduction. At 250 °C, the nickel content would still correspond to $NiNH_4PO_4 \cdot H_2O$, suggesting that the ammonium nickel phosphate compound mainly retained its structure at this temperature of reduction even if a very well-advanced amorphous character was already observed. After reduction at 500 °C, the nickel content was similar to the one expected for α-$Ni_2P_2O_7$, confirming in this case the assignment of Gopalakrishnan et al.[10] using thermogravimetric analysis. Finally, the magnetic behavior after reduction at 650 °C completely changed, showing a nearly temperature-independent paramagnetism as expected for nickel phosphide. The very low level of Ni^{2+} magnetic impurity confirmed the selective formation of Ni_2P at this temperature of reduction, as was already observed by in situ XRD and ^{31}P MAS NMR.

The following mechanism of reduction can then be proposed. Up to 250 °C, the nickel ammonium phosphate structure is essentially retained even if an amorphization process starts for $T^0 \geq 200$ °C. At 250 °C, the presence of some weak diffraction peaks of different nickel polyphosphates indicates that a dehydration process starts occurring.[37] This process is, however, quite limited, as suggested by the magnetic susceptibility measurements. After reduction at 300 °C and up to 500 °C, the decomposition of $NiNH_4PO_4 \cdot H_2O$ is effective with the formation of the α-$Ni_2P_2O_7$ pyrophosphate phase, which is formed through the following reaction:

$$NiNH_4PO_4 \cdot H_2O \rightarrow \frac{1}{2}Ni_2P_2O_7 + NH_3 + \frac{3}{2}H_2O \quad (1a)$$

As shown before, $NiHPO_4$ was not detected as an intermediate phase during the in situ XRD experiments. The intermediate formation of $NiHPO_4$ would induce two steps of dehydration and not a simultaneous elimination of NH_3 and H_2O like for the direct formation of α-$Ni_2P_2O_7$. The simultaneous detection of NH_3 and H_2O by mass spectroscopy reported by Rodriguez et al.[11] during the reduction of $NiNH_4PO_4 \cdot H_2O$ sustains the direct formation of nickel pyrophosphate.

At a temperature of reduction of 550 °C, the in situ XRD analysis showed the beginning of a crystallization process with the appearance of diffraction peaks assigned to $Ni(PO_3)_2$ and Ni_2P, while only Ni_2P was detected after reduction at 650 °C. The reduction process then occurred only for temperatures higher than 500 °C through the following reaction:

$$Ni_2P_2O_7 + \frac{17}{2}H_2 \rightarrow Ni_2P + PH_3 + 7H_2O \quad (2)$$

It is worth noting that $Ni(PO_3)_2$ was probably a secondary product resulting from the reaction of α-$Ni_2P_2O_7$ with P_2O_5 (coming from the reduction of the small $(NH_4)_2HPO_4$ impurity of the initial nickel ammonium phosphate sample):

$$2(NH_4)_2HPO_4 + \frac{1}{2}H_2 \rightarrow P_2O_5 + 3H_2O + 4NH_3 \quad (3)$$

$$Ni_2P_2O_7 + P_2O_5 \rightarrow 2Ni(PO_3)_2 \quad (4)$$

Finally, comparison of the ^{31}P MAS NMR results of our unsupported Ni_2P solid to those reported by Stinner et al.[24] for Ni_2P/SiO_2 suggests a very similar electronic environment around the P nuclei, emphasizing that the silica support did not perturb significantly the formation of Ni_2P. This was reinforced by the similar onset of reduction temperatures for our Ni_2P XRD results and those reported for Ni_2P/SiO_2 by Wang et al.[9] On the contrary, these results suggest that the different reduction mechanisms observed by Rodriguez et al.[11] between bulk and silica-supported systems are due to a too low initial P/Ni molar ratio (0.8) used during the successive impregnations of $Ni(NO_3)_2 \cdot 6H_2O$ and of $NH_4H_2PO_4$ onto silica. This would lead to the reduction of Ni^{2+} into metallic Ni^0. This phenomenon is amplified by the use of a successive method of impregnation instead of the commonly used coimpregnation technique, leading to a lower intimate contact between Ni^{2+} and phosphate groups on the support. This intermediate formation of Ni^0 reacting at higher temperature with phosphate groups would favor the formation of concomitant Ni-rich phosphide phases like $Ni_{12}P_5$ in addition to Ni_2P, which will lead to depleted HDS activity.[12] As underlined by Oyama et al.,[4] this suggests that an excess of phosphate is important in order to obtain an HDS catalyst with optimized properties. This point will be more extensively investigated in a future study about silica-supported nickel phosphide systems.

5. Conclusion

The reduction of the ammonium nickel phosphate $NiNH_4PO_4 \cdot H_2O$ precursor into Ni_2P was clarified, allowing the determination of the exact nature of the intermediate amorphous phase formed between 300 and 500 °C. Using a combination of magnetic susceptibility and in situ XRD and XAS, the amorphous phase was identified as being the nickel pyrophosphate α-$Ni_2P_2O_7$ compound. This pyrophosphate phase results from the decomposition of the ammonium nickel phosphate through simultaneous dehydration and NH_3 elimination without any reduction. Nickel phosphide (Ni_2P) was formed by the reduction of the nickel pyrophosphate between 550 and 650 °C. Therefore, this study clearly described the reduction mechanism of ammonium nickel phosphate into Ni_2P. Finally,

(37) Averbuch-Pouchot, M. T.; Durif, A. *Topics in Phosphate Chemistry*; World Scientific Publishing Co. Pte. Ltd.: Singapore, 1996.

comparison with previous studies about silica-supported nickel phosphide solids suggests that support effects did not play a significant role during the reduction process, validating our present approach. Complementary studies about silica-supported nickel phosphide catalysts will be further carried out.

Acknowledgment. H.L. thanks IFP and SIR for their financial support. We thank G. Bergeret for his help with the in situ XRD experiments and C. Lorentz for simulation of the NMR spectra.

Supporting Information Available: ^{31}P NMR spectra of the $NiNH_4PO_4 \cdot H_2O$ sample before and after reduction at 650 °C. This material is available free of charge via the Internet at http://pubs.acs.org.

IC802074K